Published by IOP Publishing for Sissa Medialab

Received: *March 14, 2023*
Revised: *October 19, 2023*
Accepted: *November 13, 2023*
Published: *December 21, 2023*

Characterization study of NaI(Tl) γ-summing spectrometer

Sathi Sharma

Department of Physics, Manipal University Jaipur, Jaipur — 303007, India

E-mail: sathisharma1994@gmail.com

Abstract: The accurate information regarding the β-decay half-life, feeding pattern from the neutron-rich nuclei have utmost importance in the field of nuclear waste management from the fission reactors as well as correct understanding about the r-process nucleosynthesis in stellar sites. The low capture cross-section measurements are also considered as major task by experimental nuclear astrophysicists. These kinds of measurements are really difficult with conventional high-resolution gamma spectroscopy techniques due to less efficiency of the detectors. For this purpose, we have an almost 4π γ-summing NaI(Tl) spectrometer at SINP, Kolkata. It is basically a cylindrical shaped detector with six sectors of NaI(Tl) crystals read by 6 photomultiplier tubes (PMT) at one end. The detailed characterization of the spectrometer via experiment using laboratory standard sources and GEANT4 simulation model to interpret all the interesting properties will be presented here in this paper.

Keywords: Detector modelling and simulations I (interaction of radiation with matter, interaction of photons with matter, interaction of hadrons with matter, etc); Digital signal processing (DSP); Gamma detectors (scintillators, CZT, HPGe, HgI etc); Scintillators, scintillation and light emission processes (solid, gas and liquid scintillators)

© 2023 The Author(s). Published by IOP Publishing Ltd on behalf of Sissa Medialab. Original content from this work may be used under the terms of the Creative Commons Attribution 4.0 licence. Any further distribution of this work must maintain attribution to the author(s) and the title of the work, journal citation and DOI.

https://doi.org/10.1088/1748-0221/18/12/P12014

2023 JINST 18 P12014

Contents

2023 JINST 18 P12014

1 Introduction

The γ-summing spectroscopy or total absorption spectroscopy (TAS) method was used primarily to measure the β-decay branching ratios, half-lives of neutron-rich nuclei and also for nuclear reaction cross-section measurements like proton and alpha capture reactions relevant for astrophysical processes. Knowledge of β-decay branching ratios, half-lives is especially important for a) nuclear model calculations tests, b) radioactive decay heat in reactors, and c) reaction network calculations for nucleosynthesis in explosive stellar events. One can produce these kinds of neutron-rich nuclei artificially in the nuclear fission reactor or they are naturally produced in stellar sites. With increasing nuclear charges in a star environment, the transmission through the Coulomb barrier dramatically declines. Due to this, charged-particle cross-sections are much too small at moderate star temperatures to account for the reported abundances of nuclides with masses more than $A \approx 60$ in the solar system. By exposing lighter seed nuclei to a neutron source, heavy nuclides ($A > 60$) can be formed. Generally, two types of neutron capture processes take place at stellar sites: (1) if the neutron flux is sufficiently small so that the β-decay constant of any unstable nucleus created after neutron capture is large compared to the decay constant of the competing (n,γ) reaction ($\lambda_\beta \gg \lambda_{n\gamma}$), it is known as slow neutron-capture process (s-process), (2) if the neutron flux is sufficiently large so that the β-decay constant of any unstable nucleus created after neutron capture is smaller compared to

the decay constant of the competing (n,γ) reaction ($\lambda_\beta \ll \lambda_{n\gamma}$), it is known as rapid neutron-capture process (r-process). As a result, the r-process will mostly yield very neutron-rich nuclei far away from the valley of β-stability, resulting in highly fragmented β-decays, i.e., many daughter nucleus states are populated with small β-branching ratio [1]. Therefore, the measurements of β-decay feeding patterns, well-understood level schemes, for which γ-summing method will play an important role, will be very effective for making detailed predictions of the r-process.

These kinds of summing detectors can also be used for total decay heat measurements at nuclear reactor facilities. The decay heat in nuclear fuel is the heat energy produced in a radioactive decay of products resulting from fission. For the design and operation of nuclear reactors, the time behaviour of this quantity is critical. It affects the fuel removal and reloading processes, safety after accidents (such as a loss of coolant incident), as well as the storage, transport, and reprocessing requirements for the spent fuel. Now, the information related to the fission yields, β-decay lifetimes, the β and γ-ray decay schemes for all of the fission products and their subsequent daughter which are decaying back to the stability line is required to calculate the time evolution of the decay heat. There are several approaches by Scientists to improve the decay heat data which can be found in the reviews of Schrock [2], Tobias [3], Tasaka et al. [4], Akiyama et al. [5] and Dickens et al. [6]. Decay heat benchmarks which are considered the standard in the field can be found in the work of Tobias et al. [7]. Works by Yoshida and coworkers [8] matched well for the gamma component of the ^{239}Pu decay heat, still there was a discrepancy in the 300-3000 s cooling time in the nuclear reactor facilities. The progress in the field of radioactive decay heat calculations reviewed in detail by Algora et al. [9]. Most of the decay heat calculations rely on data available from databases, see for example the Evaluated Nuclear Structure Data file (ENSDF) [10]. The compiled data are typically the result of the evaluation of various measurements, using various techniques, but until now they have been primarily based on the use of Ge detectors (the technique that uses Ge detectors is conventionally referred to as the high-resolution technique, because Ge detectors have a very good energy resolution). The standard approach is to compute β-decay transition probabilities for each level filled from the difference in total intensity of all γ-rays feeding the level and the sum of intensities deexciting it, compensated for the impact of internal conversion. Inevitably, this simple approach does not always yield the proper answers. If the Q-value of the β-decay is large, states having high excitation energies in the daughter nucleus can be occupied. In this situation, both the number of levels that may be directly inhabited by β-decay and the number of levels to which they can γ-decay are huge. As a result, individual γ-rays (emitted by levels with high excitation energy) have a low intensity in general. Ge detectors, and even γ-ray arrays, have poor detection efficiency, particularly at higher energies, and hence weak transitions are frequently missed in experiments. This problem was first introduced by Hardy et al. in 1977 [11] known as "Pandemonium" which stands for the problems someone faces when constructing a complex level scheme from high-resolution data in a β-decay experiment. Thus, γ-summing spectrometer that can be constructed using a large volume of detector material with high intrinsic efficiency for γ-rays, which surrounds the radioactive source in a 4π geometry plays an important role in the determination of decay heat and improving the design of the nuclear reactors.

Proton and alpha capture reactions taking place in stellar environments mostly have very low cross-sections typically microbarn ranges or even below at Gamow window region. Besides, the Q-value of most of the stellar reactions is very high, so higher energy excited states are populated in

2023 JINST 18 P12014

compound nuclei. The deexcited γ-rays have higher energy and difficult to detect using conventional high-resolution HPGe detectors specially for low intensity γ-rays. The main drawback of this kind of measurements are - larger time for data acquisition, requirement of ultra-low background and very stable targets etc. Using γ-summing technique all capture events are gathered in only one excited level, i.e., when the relevant γ-cascades feed only one state, most likely the first excited state, which is then de-excited to the ground state by a single γ-transition. As a result, the corresponding photon just gives single peak called sum-peak, of energy equivalent to the summation of all the individual energies. The large volume ensures the full absorption while allowing for the high detection efficiency [12].

Understanding the physics in γ-ray summing detectors requires detailed analysis. Thats why we need the help of Monte Carlo simulation to interpret the experimental results. So, one must characterize the γ-summing spectrometer precisely via experimental technique as well as with the help of simulation before using it in actual measurements. After that, the measurements will provide information both for the decay heat calculations used to take care of the nuclear waste from the fission reactors and on nuclei approaching the r-process, proton, and alpha induced capture cross-sections near Gamow window for astrophysics community, and new nuclear structure information for the basic nuclear physics community.

In this paper, I have characterized a big NaI(Tl) crystal made γ-summing spectrometer using experimental technique as well as via simulation whenever required. The introduction part will be followed up by γ-summing or total absorption spectroscopy methodology, details about the summing detector at SINP (Saha Institute of Nuclear Physics), Kolkata, observed important characteristics, the total γ-summing spectrum using laboratory sources (like, ^{60}Co), then GEANT4 model of the mentioned spectrometer to explain few interesting properties, summary, and future applications of this spectrometer.

2 γ-summing or total absorption spectroscopy methodology

When we are far away from the stability line, i.e., $N = Z$ line, the Q-value for β-decay is quite high. Thus, the daughter nuclei which follow the β-decay can be populated in regions of high level density and at high excitation energy. It basically results to a fragmented decay with many weak β-decay branches. Then, it is followed by multiple γ-ray decay pathways from each of the higher lying daughter levels to the daughter ground state. The identification of these weak branches is almost impossible with the conventional high-resolution γ-spectroscopy technique, as suggested by Hardy et al. [11]. So, if someone build up the level scheme using high-resolution spectroscopy data, it will be incomplete, and the feeding pattern cannot be determined correctly. Now, to get rid of the problem, one can adopt the total absorption spectroscopy or γ-summing method. Large size NaI(Tl) scintillator detectors covering almost 4π solid angle for photons (when the target is exactly at the centre of the detector), are generally used to achieve the total absorption. The large response time of the NaI(Tl) detector ($\approx$ 100 ns) helps in full absorption of the photons emitted from the cascade. This is because the photomultiplier is unable to distinguish between different photons that are emitted within small interval of time (smaller than the decay time of the detector $\approx$ 250 ns). As for example, SuN (Summing NaI(Tl)) detector developed at the National Superconducting Cyclotron Laboratory (NSCL) and manufactured by SCIONIX with cylindrical core, 16 in. in diameter and

2023 JINST 18 P12014

16 in. long, with a 1.8 in. diameter borehole along its axis [12], 4π calorimeter installed at the Dynamitron Tandem Laboratorium (DTL) of the Ruhr-Universität Bochum, Germany consists of 12×12 inch NaI(Tl) detector (BICRON) with a borehole of diameter 35 mm along its axis [13], MTAS (Modular Total Absorption Spectrometer) from Oak Ridge National Laboratory [14], DTAS (Decay Total Absorption Spectrometer) from FAIR [15], HECTOR (High EffiCiency TOtal absorption spectrometeR) from University of Notre Dame, U.S.A. [16], a $5'' \times 5''$ cylindrical detector from the Australian National University (ANU5x5) and a $6'' \times 5''$ well type cylindrical detector from the Australian Nuclear Science and Technology Organisation (ANSTOwell). Another possibility to make a total absorption spectrometer is to use large volume BGO crystals [17]. The BGO detector has higher efficiency compared to a similar volume NaI(Tl) crystal but poor energy resolution w.r.t. NaI(Tl) made summing spectrometer. In case of an ideal 4π γ-summing spectrometer, we get only one peak (known as the sum peak) which has the energy equal to the level of excitation. The main advantage of the γ-summing technique is that we need to analyze the sum peak only, not the individual γ-lines from the de-excitation. The γ-summing technique has been illustrated beautifully in figure 1. In reality, it is not possible to get a 100% efficient detector. So, the intrinsic detector properties, combined with the large number of β-feeding levels, produces a complex detector response. Thus, γ-summing method depends heavily on the Monte Carlo simulation for the unfolding of the individual β-feeding level signatures from the observed spectrum.

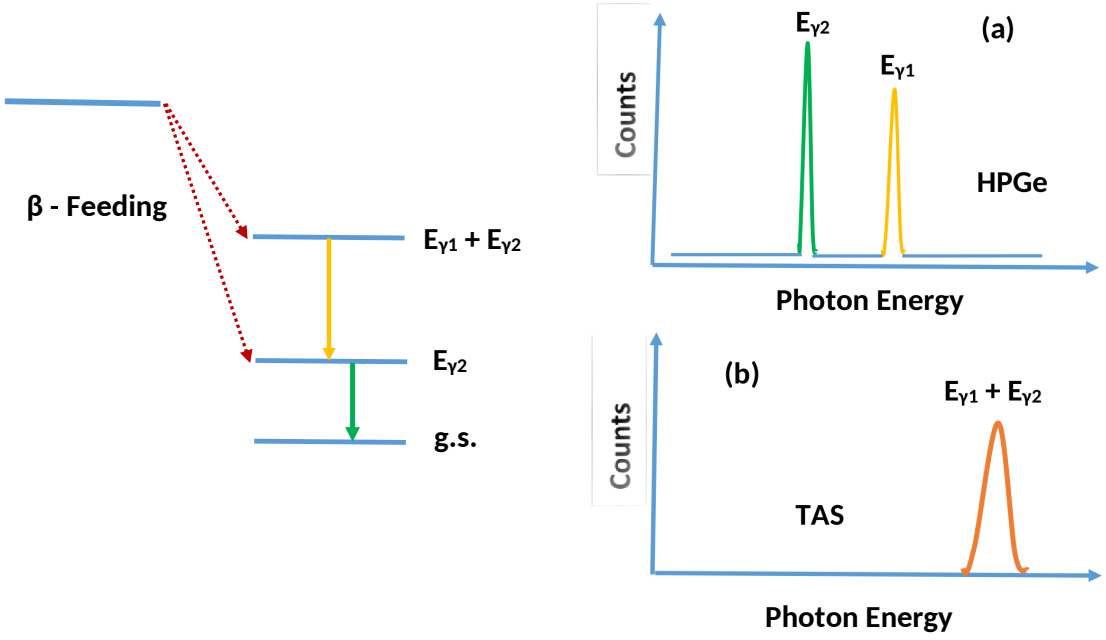

Figure 1. Decay scheme of the compound nucleus produced in a nuclear reaction (left side). Typical γ-spectra for the de-excitation of compound nucleus by using high-resolution low efficiency HPGe detector (right side marked as 'a') and a large volume 4π- summing TAS detector (right side marked as 'b'). In case of ideal 4π-detector, we get only one sum peak with energy equal to $E_{\gamma 1} + E_{\gamma 2}$. The difference between a single crystal high-resolution low efficiency detector and a summing detector has been clearly seen in this figure.

2023 JINST 18 P12014

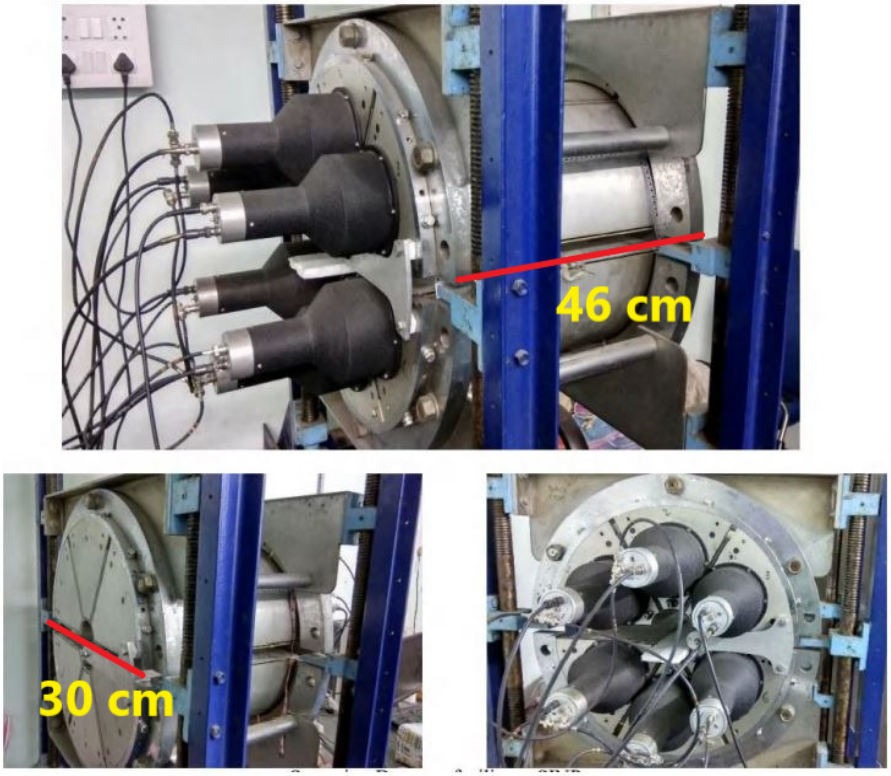

Figure 2. The γ-summing spectrometer facility at SINP, Kolkata. The six detectors with six PMTs have been seen in the figure clearly.

3 γ-summing detector at SINP

There is a large volume NaI(Tl) crystal made γ-summing detector at SINP which can be used in multiple ways. Recently, there has been a noticeable increase in the use of large NaI(Tl) detectors as total absorption spectrometers (TAS) all over the world [12, 14–16]. Before, total gamma-energy spectrometers were utilised with the huge scintillators to pick high spin states that were inhabited in compound nuclear processes. high-resolution HPGe detectors use large crystals as anti-Compton shields. These should be effective as passive shields to lower the ambient radiation in the room due to their enormous sizes. The background caused by the Compton distribution may be suppressed by a factor of 10 when they are being used [18, 19].

The detector used in the present work was manufactured by Harshaw/Filtrol in the 1980's and wasn't utilised for a long time. Without being used, it was maintained at the SINP laboratory. There was no documentation for the detector. So, the detector was recently revitalised and characterized gradually utilising various methods [20–23]. It is basically a cylindrical shaped detector with six sectors of NaI(Tl) detectors. The summing spectrometer has a length of 46 cm and a diameter of 30 cm. But, only one PMT is attached with each of the six sectors at one end of the detector, i.e., total 6 number of PMTs. There is borehole at the centre of the cylindrical assembly which has a diameter of 8 cm. The sources have been placed along the axis of the summing detector. The γ-summing spectrometer has been shown in figure 2. Each crystal is surrounded by magnesium oxide (MgO)

2023 JINST 18 P12014

reflector. The detector has a quartz window at one end of the detector with an attached bialkali photocathode. It is followed by voltage multipliers and finally the photoelectrons are collected by the anode. The anode signal is modified by the preamplifier circuits. So, we have three knobs outside each NaI(Tl) detector - one to give the high voltage, one to take the preamplifier output and another knob to change the gain of the PMT. The photomultiplier portion is covered by some black coated material which prohibits the direct light absorption by the photocathode from outside. The active volume of the NaI(Tl) crystals are totally covered by aluminium material.

Here, the initial characterization was performed using a CAEN DT5780M desktop digitizer [24, 25]. Initially, it was required to determine the optimum settings of the digitizer's parameters that resulted in the best spectrum for each of the crystals. We next investigated the plateau characteristics, or fluctuations in the spectrum with rising bias voltage, and determined the optimal bias voltage for which the detector's response is the best from the count rate vs. bias voltage curve (see ref. [20–23]). Six high voltage units are required to operate all of these detectors concurrently. However, given the current requirements of each detector, it became apparent that a single ORTEC 556 high voltage unit could deliver bias to all of them via a high voltage distribution box designed and built in SINP workshop. Using this mentioned set-up, the spectrometer was utilized as passive and active shielding to an HPGe detector inserted into the borehole [20–23]. So, first we have studied the characteristics of individual crystal which is discussed thoroughly in section 4. Later, new CAEN power supply modules and digitizer was procured to get the total summed output of the six NaI(Tl) crystals (see section 5).

4 Distinct characteristics of the spectrometer

Few important features of the summing spectrometer have been studied using laboratory standard sources like ^{60}Co and ^{137}Cs. We have used CAEN DT5780M desktop digitizer [24, 25] to give the bias voltage to the individual crystal and to acquire the energy spectra. The schematic diagram of the electronics set-up is shown in figure 3. The observations related to the resolution of the detector for a particular gamma energy as a function of bias voltage and position of the source and photo peak position w.r.t. the source position along the borehole axis is discussed below in details.

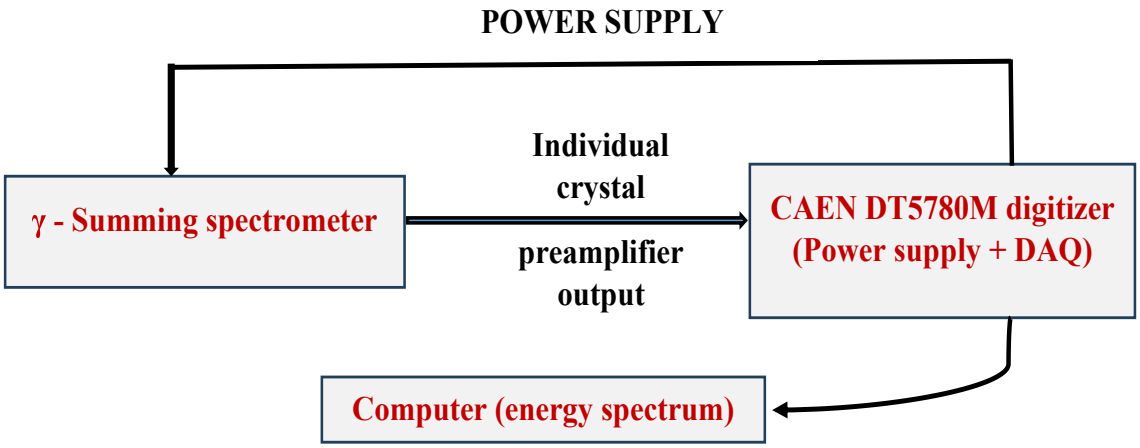

Figure 3. Schematic diagram of the electronics set-up to study the characteristics of individual crystals.

2023 JINST 18 P12014

4.1 Resolution

The resolution is an important parameter which decides the performance of any γ-ray spectrometers. The resolution of a detector depends on different parameters like bias voltage to the detector, optimization of the data acquisition parameters such as shaping time, pole zero, etc., and the position of the source especially for the case of such summing detectors with long crystals. The resolution of each individual crystal has been checked by varying the biasing voltage and the position of the γ-source. ^{137}Cs source has been used here to deduce the resolution of the detector. After plotting the resolution ($R = \frac{\text{FWHM}}{E_\gamma}$) as a function of bias voltage, we get the best resolution 12% at 662 keV. The resolution is best at 750 V and remains almost same up to 1200 V.

The resolution of the crystal also has been plotted as a function of different source positions. The data has been taken in two conditions — (1) by changing the source position along the axis of the detector, and (2) by changing the source position along the surface of the detector. One of the plots has been shown in figure 4. It can be observed from figure 4 that the resolution of the detector is almost the same around 12% at 662 keV, but gradually increases when the source's position is varied from 20 cm to 30 cm. The resolution is poorer at 25 to 27 cm. However, the resolution beyond 30 cm, decreases gradually and behaves in a same manner as it does before 20 cm. The nature of the resolution plot at two conditions are quite similar. Here, all the distances measured from the face where the PMTs are attached to the detector.

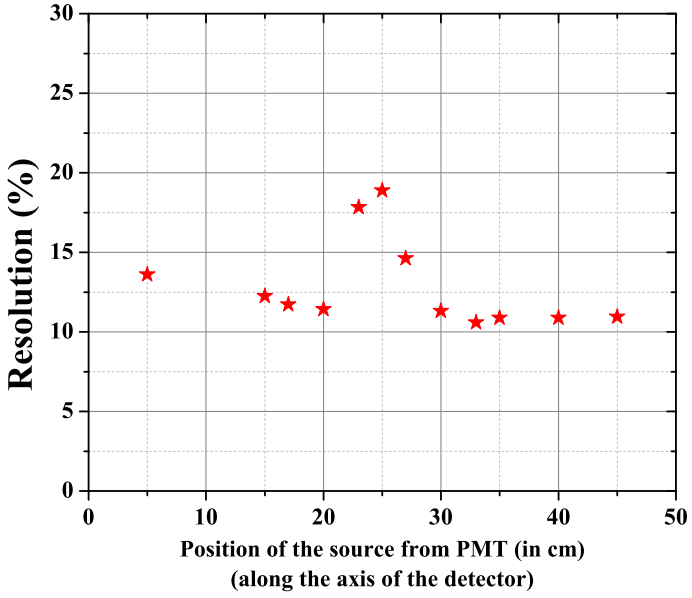

Figure 4. The resolution at different source positions along the central axis (upper one) and over the surface (lower one) for 662 keV peak from the ^{137}Cs source for one of the crystals among the six. The gradual increment in the resolution value from 20 to 30 cm has been clearly seen in the figure. The resolution is poorest at a distance of 25 cm from PMT.

4.2 Photopeak position

As mentioned above, the photomultiplier is attached to one side of the γ-summing spectrometer. So, the scintillation light collection efficiency of the photocathode varies widely as we move the

2023 JINST 18 P12014

source from the PMT. The photopeak positions of 662 keV from the ^{137}Cs source and 1173 and 1332 keV from ^{60}Co have been plotted as a function of the position of the source from PMT (see figure 5). From figure 5, it can be observed that the variation of the photopeak position is more in the higher energies compared to lower energies. The photopeak shifts towards the left side, i.e., at lower channel number (or energy) with the increase in the distance of the source from the PMT, especially after 25 cm. However, there is some anomalous behaviour in the detector response at around 25 cm. The energy spectra of ^{60}Co and ^{137}Cs at 20 cm, 23 cm and 27 cm have been compared in figure 6. It can be observed that the peaks corresponding to 1173 keV and 1332 keV are not properly resolved and distorted, as shown in figure 6. We get three humps or peaks in the case of the ^{60}Co source at 25 cm. In case of 662 keV, the peak is broad and not perfectly gaussian.

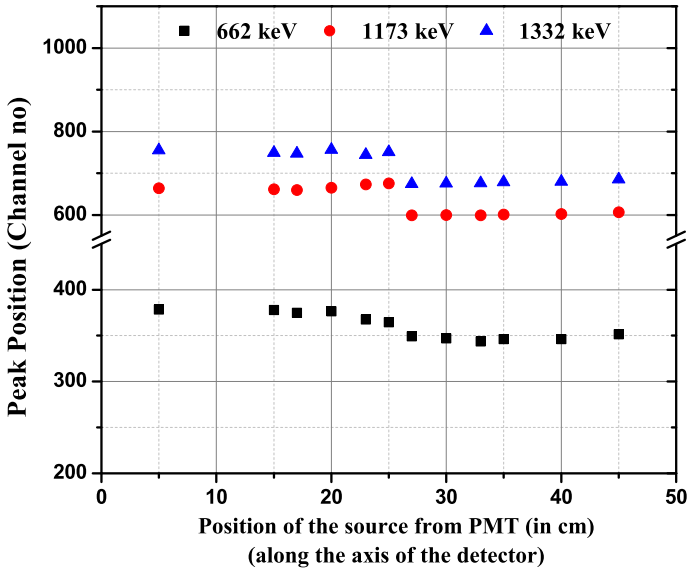

Figure 5. Position of the photopeak for different energies vs. the distance of the source from the PMT. As the distance of the source from the PMT increases, the peak position shifts to the left in the energy spectrum, i.e., the channel number decreases.

The observed phenomenon can be explained in terms of the location of the γ-photon interaction within the detector material, the length of the scintillation photons' path, the absorption of the scintillation photons by the detector material itself, and the separation between the interaction locations within the crystal and photocathode, especially when the length of the crystal is very large. Therefore, the peak amplitude, the total number of optical photons, and the energy resolution change drastically caused by path length differences of the scintillation photons as they travel from their generation points to the photocathode [26]. Here, the PMT solely on one side of the crystal is what causes the abrupt appearance of three peaks with ^{60}Co in between 20 and 30 cm. There are only two ^{60}Co peaks in the spectrum when the source is close to the PMT because the first half of the detector mostly detects γ-rays. The γ-photons are mostly gathered by the second half of the crystal if the source is placed close to the second half of the detector. As a result, the spectra remain unchanged in the lower channels despite insufficient photon collection by the γ-summing spectrometer. Now, some γ-photons are detected by the first half of the detector, and the remainder by the second half of the detector if the source is positioned in the centre of the detector. The peak signals from the two

2023 JINST 18 P12014

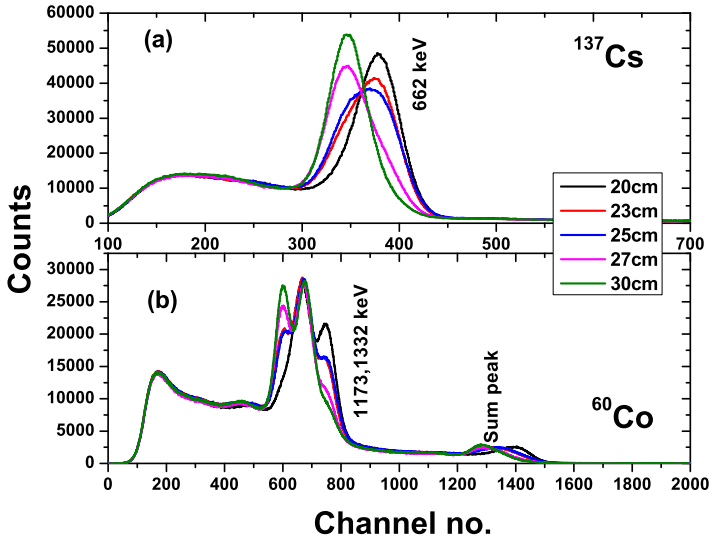

Figure 6. Energy spectra of (a) ^{137}Cs and (b) ^{60}Co when the source position is varied from 20 cm–30 cm from PMT for a single crystal. In figure 6(a), the 662 keV peak becomes non-gaussian and broad at 25 cm distance. In figure 6(b), one can observe the appearance of three humps or peaks at distances 23–27 cm.

halves of the detector, 1173 and 1332 keV, do not entirely converge. Thus, this area is experiencing three humps (see figure 6). For example, the energy spectrum of ^{60}Co at 15 cm and at 35 cm from the PMT added together. After that, it is compared with the energy spectrum at 25 cm with proper peak count normalization. Both spectra are comparable to each other. It is shown in figure 7. The red color spectrum corresponds to the energy spectrum at 25 cm and the black one corresponds to the added energy spectrum at 15 cm and 35 cm distances from PMT (see figure 7).

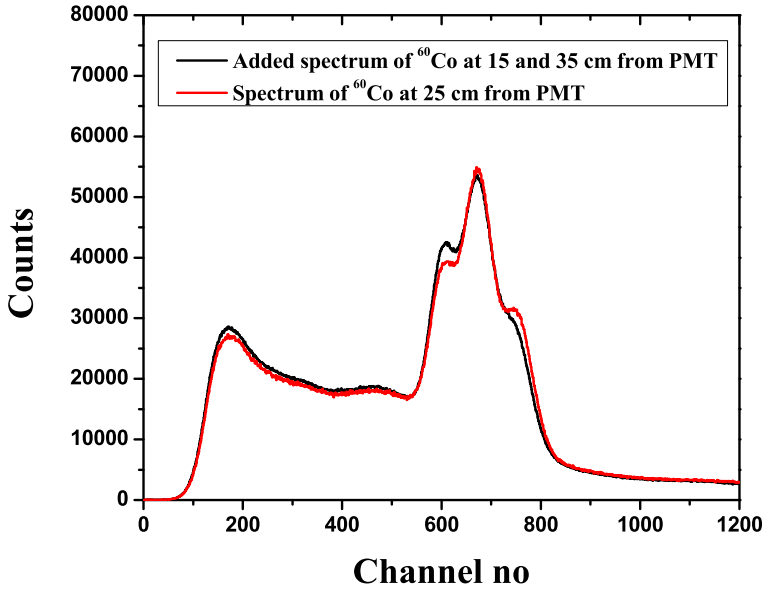

Figure 7. Energy spectra of ^{60}Co where the red one corresponds to the source position at 25 cm and the black one is the added energy spectrum at a distance of 15 cm and 35 cm respectively, from PMT.

2023 JINST 18 P12014

5 The γ-summing spectrum

To get the total spectrum using lab standard sources like ^{60}Co, first one has to match the gain of each individual PMT's using a single gamma line source (^{137}Cs) and then the responses have to be added to each other. Both methods are discussed thoroughly, one by one, below.

5.1 Gain matching

The PMT responses depend largely on the given bias voltage. If the detector has a single PMT, then there is nothing to bother. However, this is not the case for large detectors with multiple PMTs, as the final signal is the summed response of the individual sectors. Whenever one tube has higher or different gain than the rest, the total detector response will result in a poor resolution or, in the extreme case, an unrecognized spectrum. So, it is important to gain match all the PMTs before taking the total response of the detector.

To gain match the six PMTs to align the single peak positions for a fixed bias, we have used single line ^{137}Cs source. Here, we have used two power supply modules procured from CAEN – DT5533EM and DT5533EP to give the bias to each individual PMTs. The high voltage was varied to match the photopeak positions of the six sectors of the summing spectrometer. The source was placed at a distance of 12 cm from the PMT at the central axis of the summing spectrometer. The data have been acquired with DT5730 CAEN digitizer (8 channels, 14 bit, 500 MS/s) with COMPASS software [27]. The gain-matched spectra from all the six crystals are shown below in figure 8.

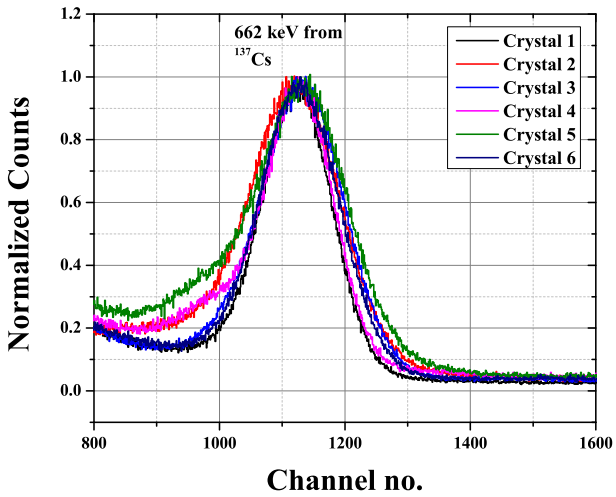

Figure 8. The gain-matched spectra from all the six crystals.

5.2 Total spectrum

The total spectrum of the γ-summing spectrometer was taken in two modes: (1) add mode and (2) addback mode. In add mode, the signals from six sectors are simply added like a daisy chain to get the added spectrum of the whole spectrometer. The schematic diagram for the electronics set-up is shown in figure 9. Next, we take the data of individual detectors in the "OR" condition in addback mode and then perform the virtual addback in COMPASS software with a 400 ns time window (see

2023 JINST 18 P12014

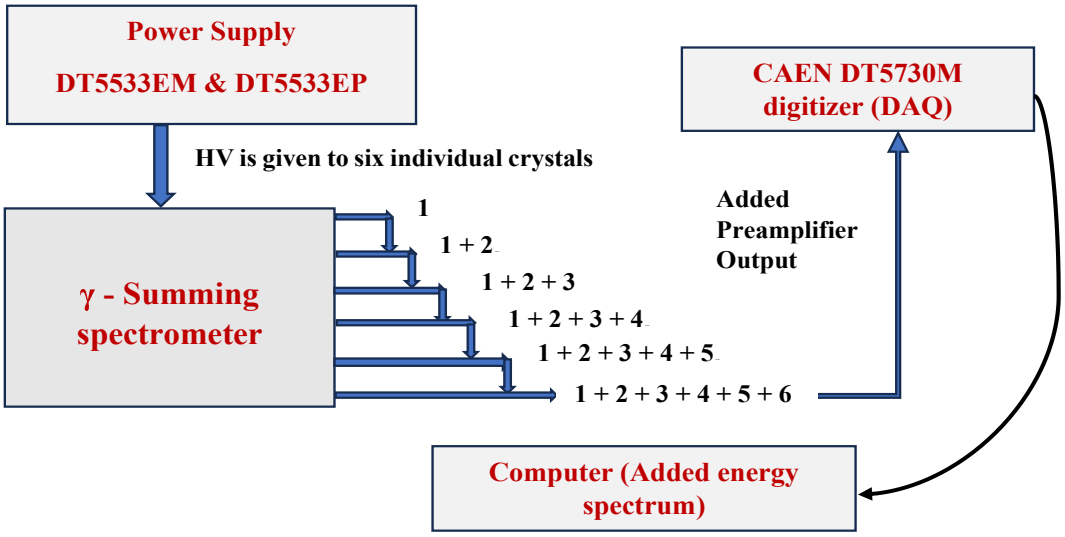

Figure 9. A schematic diagram of the electronics set-up to get the added spectrum. The individual preamplifier outputs from the six sectors are added with the help of connectors. The summed preamplifier output (1 + 2 + 3 + 4 + 5 + 6) is given to the CAEN DT5730M DAQ system. High voltage is given to six individual sectors using two power supply modules DT5533EM and DT5533EP respectively.

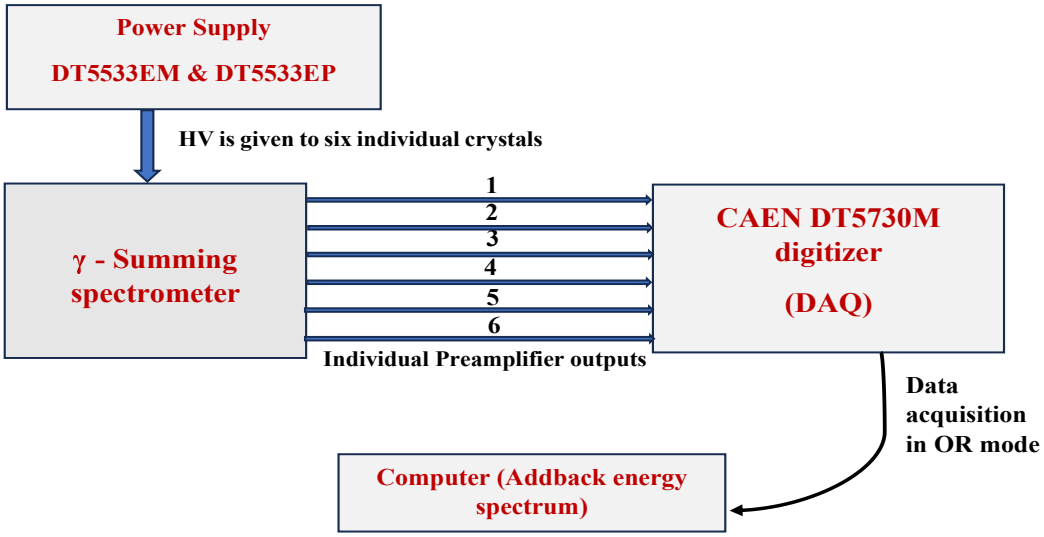

Figure 10. A schematic diagram of the electronics set-up to get the addback spectrum. The individual preamplifier outputs of the six sectors are processed simultaneously and connected to the six input channels of the CAEN DT5730M digitizer. High voltage is given to six individual sectors using two power supply modules, DT5533EM and DT5533EP respectively. The data has been taken in OR mode with 400 ns time window. After that, the acquired list mode data was sorted properly using the COMPASS software to get the addback spectrum.

figure 10). Addback is the property to get back the compton scattered data to increase the photopeak efficiency in a particular time window. At the time of data acquisition, the source has been placed at a distance of 12 cm from the PMT. The main advantage of taking the data in "OR" condition is

2023 JINST 18 P12014

that we can make the addback with different conditions like as per time window, multiplicity, etc. The total spectra in both conditions have been shown in figure 11 for ^{60}Co source. In figure 11, the summing of 1173-1332 keV peaks, i.e., sum peak of ^{60}Co is clearly observed.

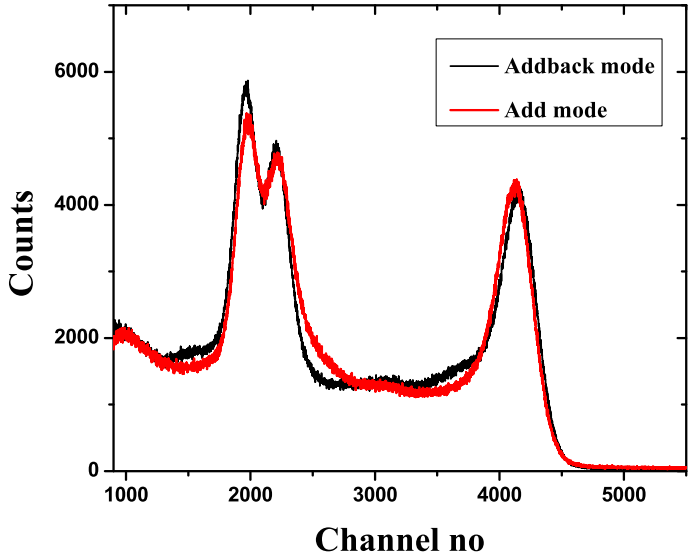

Figure 11. The total spectra of the γ-summing spectrometer at addback mode (Black color) and in add mode (Red color). The sum peak at (1173+1332) keV has been clearly observed at both the conditions.

Due to the extra loss in signals during its transmission through multiple connectors and cables or through the daisy chain connection, the threshold of the pulse height becomes high in case of add mode and count is less at lower channels compared to addback mode. So, overall, addback mode is comparatively better to use. As mentioned above, in addback mode, we can also apply different conditions, like time window, multiplicity, etc., at the time of offline analysis.

6 GEANT4 model of γ-summing spectrometer

As discussed above, the behaviour of the summing spectrometer at certain positions of the source is not completely clear. Now, the sudden change in the resolution and the peak position (as shown in figure 4, figure 5 and figure 6) of different energies may be due to the inefficient collection of scintillation photons to the photocathode from the entire volume of the detector. So, to resolve this anomalous behaviour or better understanding of the γ-summing spectrometer characteristics at certain length interval of the detector, we take the help of Monte Carlo simulation. The GEANT4 simulation toolkit [28] has been used to simulate the response of the summing spectrometer as accurately as possible. This model will be used to interpret the experimental data (like energy spectrum, efficiency, etc.), so that it needs to reproduce as many features of the detector as possible. The different components of the simulation code have been described in detail below.

6.1 DetectorConstruction

One of the main important classes in GEANT4 is the DetectorConstruction class which takes care of all the components of the detector. However, the main problem with building the models of detectors

2023 JINST 18 P12014

is related to the inability to measure the internal components, so that we must give extra efforts to construct the summing spectrometer to match the experimental data of the detector. Here, the bulk of the detector volume consists of sodium iodide (NaI) material. Then, we have a magnesium oxide (MgO) reflector which surrounds the crystal surface. The detector has a quartz window at one end of the detector with an attached bialkali photocathode. The properties of the NaI crystal like scintillation yield, time constant have been included in the simulation code. The optical properties like refractive index, absorption length have also been included in the code to directly simulate the optical photons from scintillation light. A schematic GEANT4 summing spectrometer geometry has been given in figure 12.

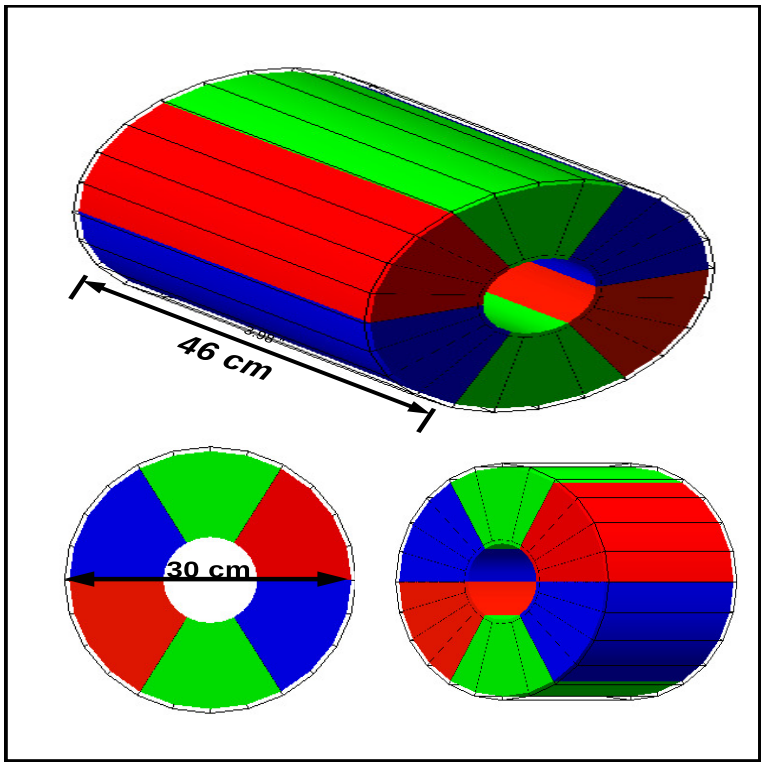

Figure 12. A schematic of the γ-summing spectrometer geometry that have been used in the GEANT4 [28] simulation.

6.2 PhysicsList and PrimaryGenerationAction

The PhysicsList class basically helps the user to define the properties and behaviour of the particles or photons which will be used in the simulation. Here, we have used the standard low-energy electromagnetic (EM) physics module. We have also included the Radioactive Decay Module (RDM) and optical physics processes here. The RDM module allows the creation of a radioactive ion as the source of particles. The data contained in the RDM input files is basically from the ENSDF database of NNDC [29].

The PrimaryGeneratorAction is a mandatory class that defines the method by which particles are generated. There are different classes to define the particles — particle gun and general particle source (GPS). The basic class particle gun can be used to define only monoenergetic particles in a defined direction. However, in GPS class, one can define the energy and direction of the emitted particles fully.

2023 JINST 18 P12014

These previously mentioned classes are followed by SteppingAction and EventAction classes. And finally, in the RunAction class, the data has been collected and written to an output file. Further analyses have been performed using the root framework [30].

6.3 Optical photon simulation

Here, we have adopted two methods to simulate the detector response: (a) energy deposition method and (b) optical photon method. In the energy deposition method, the energy loss in each step is noted using the G4Step class to calculate the total energy deposit per event. In the case of optical photon method, the light produced in the scintillator crystal. Then it tracks the photons until they hit the PMT photocathode. The photocathode is basically used to count the amount of light (number of absorbed photons) that reach the material. To investigate the fundamental reason for the observed characteristics of the summing spectrometer (like shifting of the photopeak with different source positions, anomalous behaviour in between certain lengths of the detector), we have to choose the optical photon method. Optical photon simulations can take 100-1000 times longer to complete compared to the non-light simulations. Due to this fact alone, the selection of this option for simulations is not a favourable one for general purposes, although it holds promise for a more fundamental understanding of how the summing or total absorption spectrometer works. The experimentally observed characteristic, i.e., the shifting of the photopeak positions and energy resolution as a function of source position has been simulated using the optical photon model. It is shown in figure 13. From figure 13, it is clearly observed that the optical photon model nicely reproduces the experimental spectra.

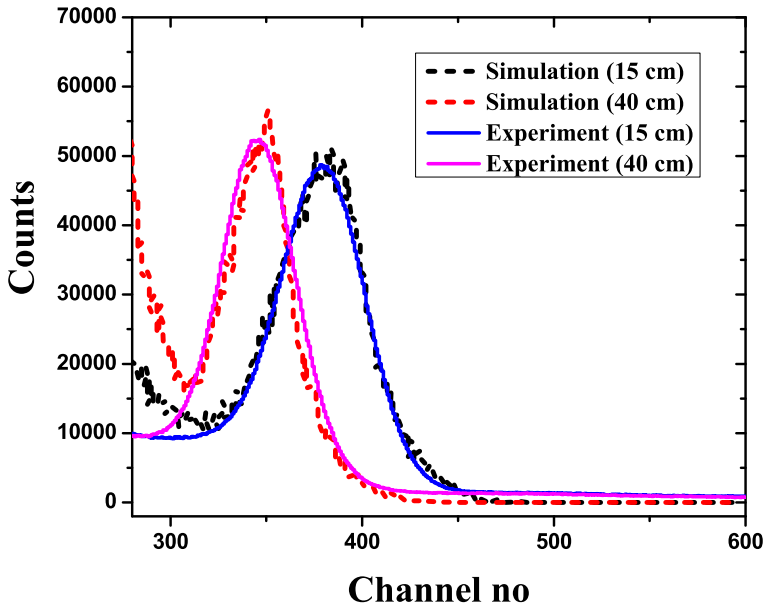

Figure 13. The shifting of the photopeak positions as a function of source position has been simulated using the optical photon model in GEANT4 [28] using the ^{137}Cs source. The source has been placed at two positions near and far from the PMT. The experimental spectra have been compared with the simulated spectra. The simulated counts are normalized with the experimental counts for better comparison.

2023 JINST 18 P12014

7 Summary and future outlook

I have presented here the γ-summing spectrometer at SINP, Kolkata. The characteristics of the spectrometer have been checked through experiment as well as using simulation. Few distinctive properties of the big spectrometer are understood properly with the help of simulation. As the summing spectrometer has PMT only on one side, we have to choose an optimum position for the experiment to maximize its efficacy. Nearly at 12 cm, we get the summing efficiency maximum with ^{60}Co source. The value of the efficiency of the sum peak for ^{60}Co at 12 cm distance from the PMT is found to be 24 (1)%. The set-up has been tested with single and double-line γ-sources like ^{137}Cs and ^{60}Co respectively. In future, I want to use multiple γ-line sources like ^{152}Eu for further characterization of the γ-summing set-up. ^{152}Eu which has comparatively longer half-life ($T_{1/2}$ = 13.537 (6) y, decays to ^{152}Gd and ^{152}Sm by β^- and ϵ decays with branching ratio of 28% and 72%, respectively. β-feeding from the parent is fragmented in a number of daughter states, with the majority of the feeding occurs in the three states at 1.09 MeV (21.7%), 1.23 MeV (17.4%), and 1.53 MeV (24.9%) in ^{152}Sm [29]. So, the experimental set-up and the simulation code can be tested for the reproducibility of the reported β-feeding intensities [31]. Later, the facility can be utilized to study more fragmented β-decays from neutron-rich nuclei. The FRENA facility [32] at SINP, Kolkata is a low-energy accelerator facility that can produce proton beams with energies ranging from 0.400 MeV to 6 MeV with high current up to several hundred µAs. The author has studied the resonance reaction of ^{14}N(p,γ)^{15}O at E_{lab} = 278 keV. This reaction has several consequences in nuclear astrophysics — from neutrino production in our Sun, to age estimates of globular clusters in our Galaxy [33]. The cross-section for the reaction drops to nanobarn to picobarn range when we move from the resonance energy. Due to that, the cross-section measurement is difficult with the conventional high-resolution γ-detectors. Thus, this summing spectrometer will be extremely useful for measuring the very low capture cross-section over a broad range of energies. So, proton capture cross-sections important for stellar nucleosynthesis can be studied effectively using this γ-summing spectrometer.

Acknowledgments

The author is grateful to Prof. Maitreyee Saha Sarkar for her kind help and cooperation throughout the work. The author appreciates the Saha Institute of Nuclear Physics (SINP) authority's kind assistance during the accomplishment of the work.

References

[1] C. Iliadis, *Nuclear Physics of Stars*, Wiley-VCH Verlag GmbH & Co. KGaA, Weinheim (2007).

[2] V.E. Schrock, *Evaluation of decay heating in shutdown reactors*, *Prog. Nucl. Energy* **3** (1979) 125–156.

[3] A. Tobias, *Decay Heat*, in *Progress in Nuclear Energy*, Elsevier (1980), p. 1–93 [DOI:10.1016/b978-0-08-027115-6.50004-6].

[4] K. Tasaka, J. Katakura and T. Yoshida, *Review of decay heat calculations*, in the proceedings of the *International Conference on Nuclear Data for Science and Technology*, Mito, Ibaraki, Japan, 30 May–3 June 1988, pp. 819–826.

2023 JINST 18 P12014

[5] M. Akiyama and S. An, *Measurements of Fission-Product Decay Heat for Fast Reactors*, in the proceedings of the *International Conference on Nuclear Data for Science and Technology*, Antwerp, Belgium, 6–10 September 1982, pp. 237–244 and references therein [DOI:10.1007/978-94-009-7099-1_51].

[6] J.K. Dickens, T.A. Love, J.W. McConnell and R.W. Peelle, *Fission-Product Energy Release for Times Following Thermal-Neutron Fission of 235U Between 2 and 14 000 s*, *Nucl. Sci. Eng.* **74** (1980) 106.

[7] A. Tobias, *Derivation of Decay Heat Benchmarks for U235 and Pu239 by a Least Squares Fit to Measured Data*, Tech. Rep. CEGB RD/B/6210/R89, 1989.

[8] T. Yoshida et al., *Possible Origin of the Gamma-ray Discrepancy in the Summation Calculations of Fission Product Decay Heat*, *J. Nucl. Sci. Tech.* **36** (1999) 135.

[9] A. Algora and J. L. Tain, *Decay Heat and Nuclear Data*, in *Nuclear Reactors*, InTech (2012) [DOI:10.5772/34622].

[10] http://www.nndc.bnl.gov/ensdf.

[11] J.C. Hardy, L.C. Carraz, B. Jonson and P.G. Hansen, *The essential decay of pandemonium: A demonstration of errors in complex beta-decay schemes*, *Phys. Lett. B* **71** (1977) 307.

[12] A. Simon et al., *SuN: Summing NaI(Tl) gamma-ray detector for capture reaction measurements*, *Nucl. Instrum. Meth. A* **703** (2013) 16.

[13] A. Spyrou et al., *Cross-section measurements of capture reactions relevant to the p process using a* 4π *γ-summing method*, *Phys. Rev. C* **76** (2007) 015802.

[14] M. Karny et al., *Modular total absorption spectrometer*, *Nucl. Instrum. Meth. A* **836** (2016) 83.

[15] V. Guadilla et al., *Characterization and performance of the DTAS detector*, *Nucl. Instrum. Meth. A* **910** (2018) 79 [arXiv:1806.01138].

[16] C.S. Reingold et al., *High Efficiency Total Absorption Spectrometer HECTOR for capture reaction measurements*, *Eur. Phys. J. A* **55** (2019) 77.

[17] C. Casella et al., *A new setup for the underground study of capture reactions*, *Nucl. Instrum. Meth. A* **489** (2002) 160.

[18] S. Sharma and M. Saha Sarkar, *Measurement and simulation of gamma-ray background in a low energy accelerator facility*, 2020 *JINST* **15** T09003 [arXiv:2004.13759].

[19] M. Saha Sarkar et al., *Characterization of NaI(Tl) Sum Spectrometer and its utilization*, *Proc. DAE-BRNS Symp. Nucl. Phys.* **61** (2016) 1022.

[20] S. Datta, *Characterization and rejuvination of large NaI(Tl) detetors with CAEN digitizer*, M.Sc. Project, Banaras Hindu University, Work done at Saha Institute of Nuclear Physics, 2016, unpublished.

[21] T. Mitra, *Optimization and position dependance of source for a large NaI(TI) detector*, M.Sc. Project, Banaras Hindu University, Work done at Saha Institute of Nuclear Physics, 2016, unpublished.

[22] H. Rattan and P.P. Das, *Characterization of large NaI(Tl) scintillation detector*, BS-MS Project, IISER Kolkata, Work done at Saha Institute of Nuclear Physics, 2018, unpublished.

[23] R. Gupta, *Large NaI(Tl) gamma-ray Sum Spectrometer for measurements of reaction cross-sections*, Post-M.Sc. Project, Saha Institute of Nuclear Physics, 2018, unpublished.

[24] C. Tintori, *WP2081 Digital Pulse Processing in Nuclear Physics*, Rev. 2.1, 2011;

[25] *UM2606 DT5780 Dual Digital MCA User Manual*, Rev. 4.

2023 JINST 18 P12014

[26] W.W. Moses, W.-S. Choong and S.E. Derenzo, *Modeling Time Disersion Due to Otical Path Length Differences in Scintillation Detectors*, *Acta Phy. Polon. B Proc. Suppl.* **7** (2014) 725.

[27] *User manual UM5960, CoMPASS, Multiparametric DAQ Software for Physics Applications*, Rev. 8, 13 March 2019.

[28] GEANT4 collaboration, *GEANT4 — a simulation toolkit*, *Nucl. Instrum. Meth. A* **506** (2003) 250.

[29] http://www.nndc.bnl.gov.

[30] R. Brun and F. Rademakers, *ROOT: An object oriented data analysis framework*, *Nucl. Instrum. Meth. A* **389** (1997) 81.

[31] G. Mukherjee et al., *A Unique TAS Setup for high multiplicity events at VECC, Kolkata using BaF_2 detectors*, *EPJ Web Conf.* **66** (2014) 11026.

[32] https://www.saha.ac.in/web/frena-about-frena.

[33] S. Sharma et al., *Proton capture resonant state of ^{15}O at 7556 keV*, *Phys. Rev. C* **102** (2020) 024308 [arXiv:2006.12371].

2023 JINST 18 P12014